Vol. 14, No. 39, Summer 2024, pages 69-79

Journal of Analytical and Numerical Methods in Mining Engineering

Journal home page: http://anm.yazd.ac.ir/

Research article

The effect of Basalt fiber and PVA-Resin additives on the Gamma-ray shielding and permeability performance of clay-liners

Afsaneh Haghshenas[1], Hajar Share Isfahani[1], Sayyed Mahdi Abtahi[1], Amin Azhari[2]*

1- **Dept. of Civil Engineering, Isfahan University of Technology, Isfahan, Iran**
2- **Dept. of Mining Engineering, Isfahan University of Technology, Isfahan, Iran**

*Corresponding author: E-mail: *aazhari@iut.ac.ir*
(Received: *December 2023*, Accepted: *July 2024)*

DOI: 10.22034/ANM.2024.20991.1618

Keywords

Bentonite clay
Radiation shielding
Gas permeability
Hydraulic permeability
Radioactive waste disposal

Abstract

In recent decades, with the growth of population and the development of metropolitans around the world, the issue of landfill and waste management has become more and more critical. Due to development of radioactive material applications, disposing these radioactive waste material became an important geo-environmental concern. Bentonite clay as an eco-friendly and natural shielding material is used as the main material for landfill barriers. The radiation shielding performance of bentonite clay modified by different percentages of basalt fiber and Polyvinyl alcohol (PVA) resin additives is investigated using experimental measurement, Monte Carlo N-Particle (MCNP) simulation, and XCOM database methods, in Gamma-ray energy levels of ^{60}Co (1173.2 and 1332.5 keV). The employed sample mixtures include 0.25, 0.5, 1, and 2 percent of basalt fiber and PVA resin additive. The obtained results for Gamma-ray shielding measurement from these three methods have a good agreement, depicting an increasing trend in the linear attenuation coefficient for higher percentages of additives. The maximum increment is observed at 0.5 percent of additive, from 7.85 to 9.69 m^{-1}, and 9.3 to 11.23 m^{-1}, in energy levels of 1132.5 and 1173.2 keV, respectively. This improvement may decrease the bentonite clay Gamma-ray barrier thickness (half-value layers (HVL), tenth value layers (TVL)), up to 20 and 23 percent for 1173.2 and 1332.5 keV, correspondingly. Moreover, the hydraulic and gas permeability of the mixtures are controlled to find the standard and optimum mixture. In which the 0.5 to 1.0 percent of additives will keep the permeability requirement in an allowable and preferable range.

1. INTRODUCTION

In recent decades, with the growth of population and the development of metropolitans around the world, the issue of landfill and waste management has become more and more critical. Because the increasing population will lead to more waste generation and will severely affect human life and the environment.

One of the most hazardous waste products to the environment, humans, and all living beings, is low-level radioactive waste. Due to the various and modern applications of radioactive materials in industry, agriculture, and medicine, the use of these materials is increasing [1-4]. The low-level waste is treated as far as possible and then buried in the surface landfills [5]. For Low-level radiant waste disposal to reduce the threats to the environment and humans, as well as to prevent contamination of groundwater and surrounding soils, applying impermeable liners against gamma-ray, radon gas, and water is essential to cap and cover the disposal [6-11]. Bentonite is a clay containing mainly of smectite minerals, usually formed by decomposition of volcanic ash

or tuff, or occasionally from other igneous or sedimentary rocks. Bentonite clay used to be one of the best options for low-level landfill liners due to its desirable features such as abundance, reasonable price, low permeability, self-healing ability, and high retention [12-16].

Several pieces of research have been carried out to evaluate the performance of soil in the field of radiation shielding as an important characteristic for liner of low-level radioactive waste disposal.

Experimental and theoretical research was performed by Olukotun et al. to examine the gamma-ray shielding capability of two clay materials (ball clay and kaolin) [17]. The linear attenuation coefficient was obtained at photon energies of 609.31, 1120.29, 1173.20, 1238.11, 1332.50, and 1764.49 keV from Bi214 and ^{60}Co sources. The results revealed that these two clay materials had an acceptable performance in gamma-ray shielding. The experimental results agreed with the results obtained from the XCOM database.

Singh and Badiger evaluated the gamma and neutron ray shielding performance of mixtures of soil samples such as clay, clay-loam, loam, sandy-clay-loam, and sandy-loam [18]. The results indicated that loam-clay is the best radiation shielding material between all samples in this study, based on its high mass attenuation coefficient.

Akbulut et al. in experimental research evaluated the radiation shielding operation of silica fume, clay, and cement in different soil mixtures including micronized clay–white cement, clay–silica fume, gypsum, gypsum–silica fume, cement, white cement, white cement–gypsum, white cement–silica fume, cement–silica fume, red mud–silica fume, red mud, and silica fume [19]. According to values of linear attenuation coefficient of samples, clay especially clay-white cement mixture has an excellent performance in radiation shielding in comparison with other samples in this research.

Generally, literature indicated that clay soil has suitable performance in radiation shielding. To improve the clay soil efficiency in radiation shielding, the effect of different additives have been investigated. In 2016, Mann et al. investigated the effect of fly ash on the gamma-ray shielding properties of clay bricks [20]. In this research, different samples were made of natural clay with 10%, 20%, 30%, 40%, and 50% of fly ash and were tested at three levels of energies 661.6, 1173.2, and 1332.5 keV. According to the obtained results, the performance of clay fly ash bricks in radiation shielding for moderate energies was satisfactory. These bricks were suitable and eco-friendly in comparison with conventional clay bricks used for construction.

Hager et al. recently studied the improving performance of ground and pressed bentonite at 150 bar pressure [21]. The sample was coated with polyvinyl alcohol polymer (PVA), in order to reduce leakage of nuclear waste from the porosity of the bentonite. Experimental results showed that the mass attenuation coefficient for the pressed bentonite is 1.5 times greater than the coefficient of natural bentonite.

Basalt is an extrusive igneous rock made from the rapid cooling of lava at Earth's Surface. Basalt is composed of minerals including plagioclase feldspar, olivine, pyroxene, quartz, hornblende, and biotite [22]. Different types of basalt have been utilized as an additive to improve the radiation shielding performance.

In 2020, the effects of adding basalt fiber additives including 0.5, 1, 2, and 5 percent on the bentonite clay radiation shielding performance, has been studied using experimental and simulation methods. Also, the permeability of the mixtures is measured to be in the acceptable range as a vibrant parameter for radioactive disposal barriers. Results show that adding basalt fiber increases the clay-basalt mixture attenuation coefficient around 2 percent, in different levels of gamma ray energies.[23]

Moreover, another research has been carried out by Dole et al., 2002, on the gamma-ray shielding performance of a densified concrete with dense material such as basalt [24]. The results showed a significant decrease in the half-value thickness (HVT) of this new concrete type.

Li et al., 2017, evaluated the effect of basalt fiber reinforced with epoxy matrixed on the shielding performance of structural composites [25]. The results indicated that the mass attenuation coefficient increases for energy levels ranging from 31 to 80 keV and slightly increases for energy levels ranging from 356 and 662 keV. The results were also verified using the XCOM database.

Hydraulic and gas permeability is another important property for liner of radioactive waste disposal. To prevent of contamination of surface and underground water, disposal liner material should be relatively impermeable.

Thyagaraj and Soujanya, 2017, in a study, examined the hydraulic conductivity of polypropylene fiber-reinforced bentonite as a waste containment barrier [26]. In this research, bentonite with 3% of fiber content is used. The results showed that adding fiber led to a slight

increase in the hydraulic conductivity of bentonite. However, the hydraulic conductivity values of reinforced and unreinforced bentonite were in the same order of magnitude (10-10 m/s).

Experimental research was performed by Kalkan, 2013, to investigate the effect of a silica fume-scrap rubber tire fiber mixture on the hydraulic conductivity of natural soil [27]. In this research samples with scrap rubber tires and length ranging from 5 to 10 mm, thickness ranging from 0.25 to 0.5 mm and width ranging from 0.25 to 1.25 mm with the content of (1, 2, 3, and 4 %) and silica fume content of (10-20) weight percentage of natural clay were made. The results indicated that fiber modification increased the hydraulic conductivity of natural clay, but silica fume decreased hydraulic conductivity, and silica fume-scrap rubber tire fiber did not show a significant influence on hydraulic conductivity.

Ayothiraman and Singh, 2017, performed a study to improve clay properties with a basalt fiber additive [28]. In this research, different weight percentages of the fiber content, 0.5%, 1.0%, and 1.5% were considered. The results revealed that the addition of fiber improved the shear strength of soil but led to an increase in water permeability. This increase was explained by water flow through the interface of fiber and soil, in which the fiber improved the flow path for water in the soil.

A study was carried out by Moon et al., 2008, to evaluate the effectiveness of compacted soil as a barrier layer in landfills [29]. In this research, the permeability of gas and water was examined. Measured gas permeability was a magnitude of two or three orders greater than hydraulic permeability. The difference between these values for gas and water is explained by gas viscosity which made gas more permeable and soil-water interaction, which prevented water flow and reduced the permeability of water.

Another research was performed by Juca and Maciel, 2006, to determine the effective parameter in air permeability of soils [30]. Results indicated that density and degree of saturation have a significant influence on the air permeability coefficient. For samples that had been compacted in optimum water content, the air permeability value was less than samples with lower density. Furthermore, the air permeability was significantly decreased for the water degree of saturation above 85%.

The main goal of this research is to investigate the performance of bentonite clay mixed with basalt fiber and PVA-resin as a low-level radioactive waste disposal barrier. In this regard, the radiation shielding performance of modified bentonite with considered additives is evaluated using experimental and simulation methods. Moreover, hydraulic and gas permeability limitations as the landfill cover required standards are controlled.

2. MATERIALS AND METHODS

2.1. Bentonite Clay, Basalt Fiber, And Pva Resin

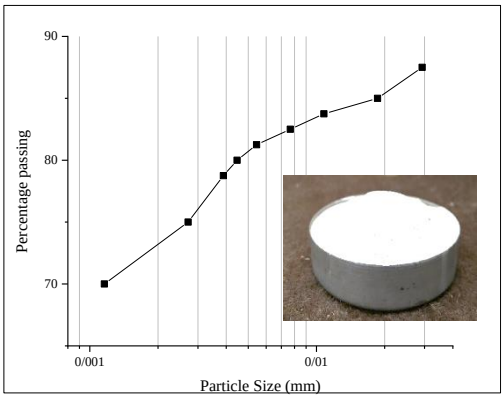

Fig. 1. The particle grading curve of utilized sodium-bentonite.

In this section, the properties of the employed bentonite clay as the base material, basalt fiber, and PVA-resin as the selected additives are presented.

• Bentonite Clay

The bentonite clay is employed as the base material due to its suitable characteristics such as low permeability, swelling ability, and self-sealing required for landfill cover layer. Bentonite clay generally consists of montmorillonite minerals [31]. The grading curve of the used bentonite is illustrated in Fig. 1 according to ASTM D422-63. The figure indicates that the grain sizes are predominantly less than 0.075 mm, with a specific gravity of 2.65 gr/cm3.

The bentonite microstructure is illustrated in Fig. 2, obtained from Energy Dispersive X-ray (EDX) analysis and Scanning Electron Microscope (SEM).

• Basalt Fiber

Basalt fiber can be produced by melting crushed basalt rocks at 1400°C and drawing the molten material. This type of basalt product has better mechanical and physical properties compared to other basalt products (i.e., glass fibers) as such, excellent resistance to chemically active environments, fire resistance, vibration, and acoustic insulation capacity [32]. The improved facilities and quality control of the basalt fiber production provided a low variability of properties and high quality [33-35].

The mechanical properties of typical basalt fiber are presented in Table 1, and the SEM image from the used Basalt fibers is illustrated in Fig.3.

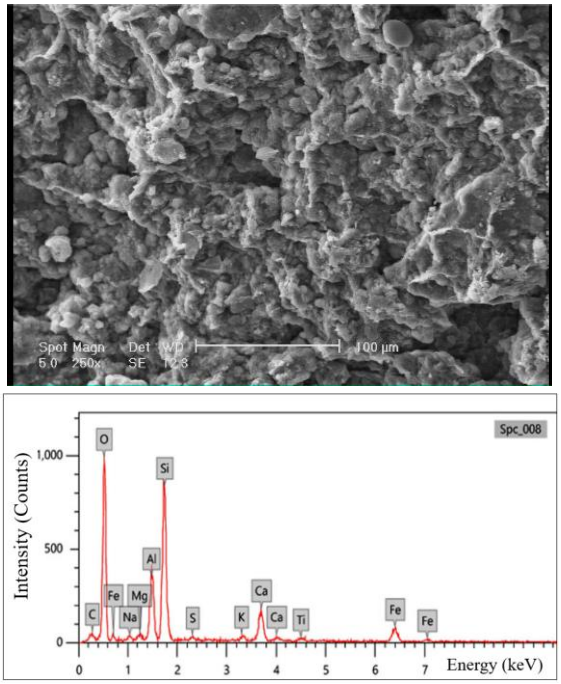

Fig. 2. SEM image and EDX analysis of the employed bentonite clay.

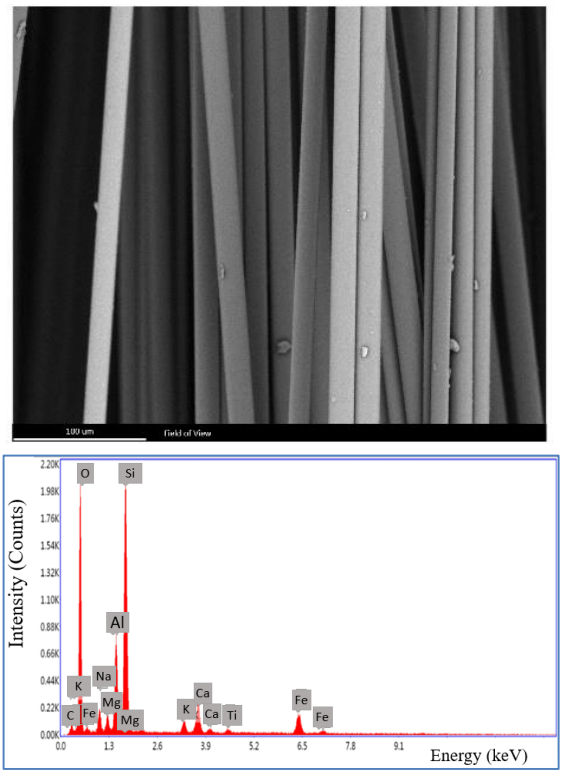

Fig. 3. SEM image and EDX analysis of the employed basalt fiber.

Table 1. Mechanical properties of a typical basal fiber

Property	Tensile strength	Elastic modulus	Elongation at break	Density
Value	*2.8–3.1GPa*	85–87 GPa	*3.15%*	2.67 g/cm^3

• Polyvinyl Alcohol (PVA)

Polyvinyl alcohol (PVA) is a water-soluble synthetic resin, which is a dry solid and is available in granular or powdered form. Recently, polyvinyl alcohol (PVA) and basalt fibers have been investigated in some construction materials such as concrete and verified their use as a suitable candidate for concrete improvement due to outstanding enhancement in their mechanical properties [36-38].

2.2. Sample Preparation

Due to the effect of moisture content and density of soil samples on the radiation shielding performance, firstly, the compaction test, according to ASTMD698 standard, is done for all considered mixtures in this study, and samples with optimum moisture content and density are prepared for the study. To prepare the samples, the utilized PVA is first mixed with water. Table 2 presents considered mixtures and their corresponding percentages of additives along with their optimum moisture and densities. Moreover, the chemical analyses (EDX) are obtained and presented in Table 3 for the mixtures.

The radiation shielding test samples for different considered mixtures are prepared with attention to the compaction test results (including optimum moisture content and its corresponding specific gravity). In this test, specimens are made in three heights of 2, 4, and 6 centimeters in a cylindrical cover with a 3.6 cm diameter (Fig. 4). To prepare the specimens, the fibers are scattered and stained with the PVA resin and a small amount of water. Then the soil is mixed with the fibers, and water is added to reach the optimum moisture with a homogenous texture. The mixture is poured into the mold and shattered with a 162g hammer to achieve the desired height. The sample is extracted from the mold and weighted.

Table 2. The optimum moisture and density for the studied mixtures

Mixture Name	Basalt Fiber %	PVA resin %	W_{opt}%	Density (kN/m^3)
BC	-	-	28	15.9
BCBFR0.25	0.25	0.25	30	16.4
BCBFR0.5	0.5	0.5	33	16.7
BCBFR1	1	1	38	16.9
BCBFR2	2	2	42	16.8

Table 3. Chemical analysis of clay, basalt fiber and their mixtures

Sample	Atomic%									
	O	Al	Si	Ca	Fe	Na	Mg	S	Cl	K
BC	42.8	8.39	41.51	3.55	3.75	-	-	-	-	-
BCBFR0.25	48.77	6	27.85	4.11	2.36	4.04	1.14	3.14	2.45	0.13
BCBFR0.5	48.92	6.11	29.66	3.89	2.6	3.3	0.95	2.87	1.56	0.14
BCBFR1	47.67	6.93	29.85	3.72	4.2	3.28	1.07	2.3	0.69	0.3
BCBFR2	49.55	6.29	28.84	4.75	3.43	2.72	1.07	2.87	0.22	0.26

Fig. 4. The prepared cylindrical samples with 3.6 cm diameter and 2, 4, and 6 cm height.

2.3. Gamma-Ray Shielding

• Radiation Shielding Theory

In physics, releasing energy in the form of particles or waves is named radiation. Ionizing and non-ionizing are two radiation categories based on the radiated particles' energy. Ionizing radiation can break chemical bonds and ionize atoms and molecules due to a high energy level. The low-level radioactive waste materials are a common source of ionizing radiation that radiates α, β, or γ rays. Because the gamma-ray is a compound of photons without mass and electric charge, its energy for penetrating and damaging living organisms is more than alpha or beta radiation. Therefore, the gamma-ray shielding is usually considered for shielding barriers [39].

In general, the performance of radiation shielding material is represented by the linear attenuation coefficient (μ). A higher linear attenuation coefficient (μ) leads to better performance of shielding, thus a thinner radiation shielding barrier layer. According to Lambert-Beer law for homogeneous shield material, the μ is derived using an Eq. (1) [40].

$$I = I_0 e^{-\mu t} \quad (1)$$

where, I_0 and I are gamma-ray intensity without a barrier sample and gamma-ray intensity transferred through a barrier sample, respectively. Also, "t" is the thickness of the radiation shielding specimen. Eq. 2 is then rewritten from Eq. 1.

$$\ln\left(\frac{I}{I_0}\right) = -\mu t \quad (2)$$

Moreover, the half-value layer (HVL) and the tenth value layer (TVL) are defined as the thickness of radiation shielding material required to reduce the incident intensity of the Gamma-ray to half and tenth of its primary values, respectively. These two parameters can be derived from Eq. 3 and 4 [41]:

$$HVL = \frac{Ln(2)}{\mu}\ (m) \quad (3)$$

$$TVL = \frac{Ln(10)}{\mu}\ (m) \quad (4)$$

• Radiation shielding measurement

Based on the mentioned radiation shielding theory, to calculate the linear attenuation coefficient (μ), the radiation intensity before and after passing from the shielding samples with different thicknesses (I_0 and I, respectively) is measured. Then, the graphs of $ln(I_0/I)$ versus the sample thickness (t) are plotted. In this research, this procedure is done using the Na-detector, shown in Fig. 5. In this research, the three commonly-used energy levels are radiated to the samples by the ^{60}Co (1173.2 and 1332.5 keV) as the radiation sources.

• Simulation and theoretical calculation of radiation shielding

Monte Carlo N-Particle (MCNP) simulation code and XCOM database are used to estimate the radiation shielding performance of the prepared sample mixtures.

The MCNP code is a computer code used to estimate the photon absorption by each barrier, which tracks the particles over a wide range of energy levels and different radiation procedures. In this statistical method, the geometry, gamma-ray source type, energy levels, and materials are defined.

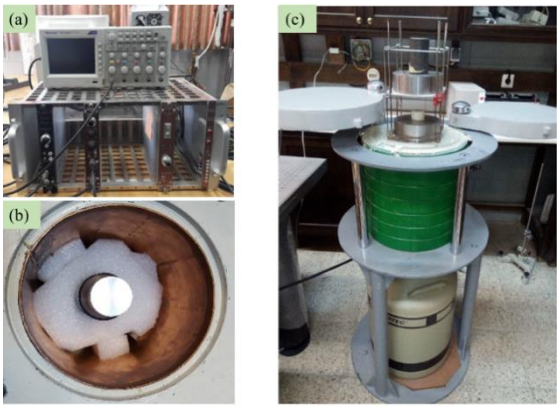

Fig. 5. Experimental radiation shielding test setup (a) computing unit, (b) Na- detector, and (c) radiation shielding measurement test setup.

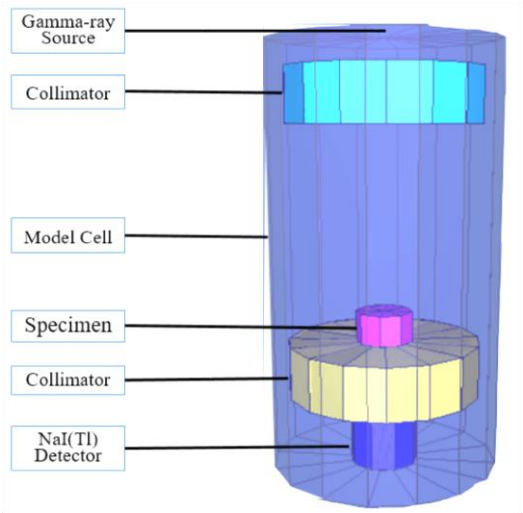

Fig. 5. The three-dimensional view of the MCNP models.

Then, a cluster of radiation is shot to the sample and follows it, regarding different states that may occur for each ray, such as scattering, absorption, or attenuation, the transmitted intensity (I) of gamma rays for the sample is calculated and the procedure is repeated without inserting the sample to define the incident intensity (I_0). Afterward, the linear attenuation coefficient (μ) is calculated using the Beer-Lambert law (Eq. 2).

In addition to the MCNP simulation, the XCOM web-based program is also used to determine the attenuation coefficient of the mixtures. XCOM is a database used to calculate photon cross-sections for total attenuation coefficients scattering, photoelectric absorption, and pair production, at energies from 1 keV to 100 GeV, in any element, mixture, and compound [42]. Fig. 5 illustrates the three-dimensional view of the MCNP models.

2.4. Hydraulic Permeability

The permeability coefficient (k) is the parameter representing the effect of soil porosity on water flow through soil structure. This parameter is a function of the fluid properties, porosity, and saturation ratio. In the unsaturated state, not only a portion of the water amount will fill the voids, but also, the friction between water and porosity walls will waste the water energy. Therefore, the maximum permeability will occur in the saturated state. In this research, the permeability of bentonite clay is measured based on the ASTM D5856-15 standard. According to this standard, the specimen is first saturated under 2 meters of persistent water head, until the discharge volume rate becomes constant. Then, due to the very low permeability of bentonite clay (around 10-11 m/sec), a 3 bar pressure is applied to the specimen. The discharge volume is then measured in a specific period until the discharge volume reaches constant. Fig. 5. illustrates the hydraulic permeability test setup. The permeability coefficient is calculated using the equation below:

$$K = QL/Ah \quad (5)$$

where, Q is the discharge volume per time (m^3/sec), L (m) is the length and A (m^2) is the section area of the specimen, and h is the applied water head (m).

Fig. 6. The setup of hydraulic permeability test (a) Hoek cell, (b) applied water head input, (c) Water discharge.

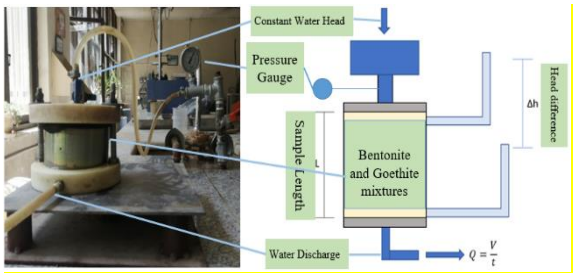

Fig. 6. Actual and schematic setup of the hydraulic conductivity test.

2.5 Gas Permeability

As noted above, permeability is related to the fluid and the medium characteristics. The permeability that is considered only as a function of the passing medium characteristics, such as porosity and friction, it would be called absolute permeability.

To measure the gas permeability, the Hoek cell from the tri-axial stress test is used. The testing setup is shown in Fig. 7. The specimen is placed inside the cell, and two porose rock cylinders are located on top and bottom of the specimen in a gasket. The gasket is filled with water, and a 50 kPa confinement stress is applied around it to avoid fluid passing around the specimen and make

sure the flow passes through the specimen. Then the airflow is inserted from the top of the cell using a gas tank, and the air discharge is measured per time through the gauge installed on the gas tank. The absolute permeability coefficient is calculated by the equation below,

$$K_{abs} = [\frac{2.30Vh\mu_a}{A(P_a + \frac{P_0}{4})}][\frac{-log_{10}^{(\frac{P_t}{P_0})}}{t}]) \quad (6)$$

where K is the absolute permeability; Pa the atmosphere pressure; P_0 is the pressure at t=0 (7 kPa); Pt is the pressure at time=t; V is the gas tank volume (m^3); H is the specimen height (m); A is the specimen section area (m^2); and μ_a is the gas dynamic viscosity at 20°C.

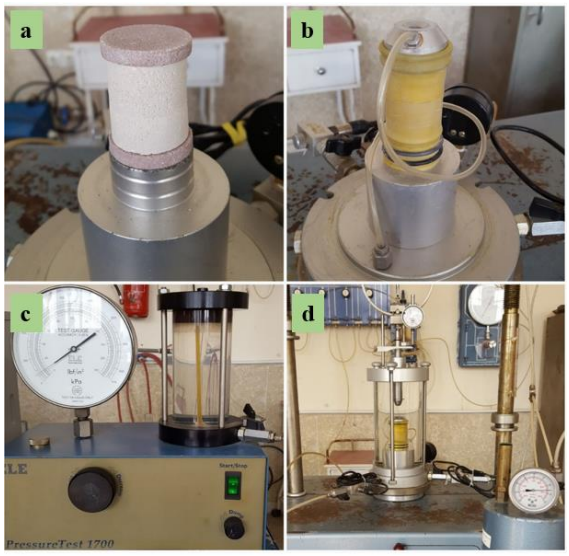

Fig. 7. The gas permeability testing setup: (a) created specimen, (b) specimen fitted in the gasket with the confinement, (c) the gas gauge, and (d) overlook of the setup.

The radiation shielding performance of the five mixtures is evaluated using the experimental test, MCNP code, and XCOM web program. As mentioned, the 1173.2 keV and 1332.5 keV energy levels are radiated using the ^{60}Co as the radiation source in the experiment. The output radiation intensity is measured using Na-detector, and the $\ln(I_0/I)$ versus sample thickness (t) is graphed in Figs. 8 and 9 for 1173.2 and 1332.5 keV levels of gamma-ray energy, respectively. According to Eq. 1, the slope of the linear fit to these graphs would be the linear attenuation coefficient (μ). Moreover, the linear attenuation coefficients obtained from the three experimental, MCNP, and XCOM approaches, are presented in Table 4.

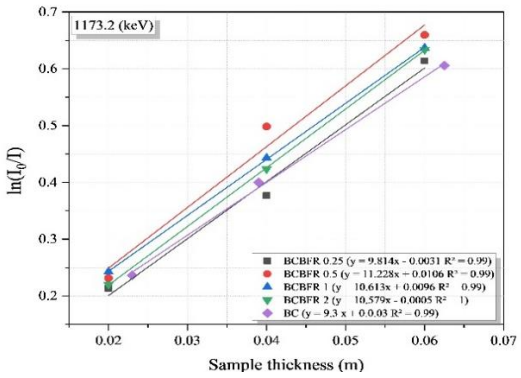

Fig. 8. The ln(I0/I) versus sample thickness (t) at 1173.2 keV.

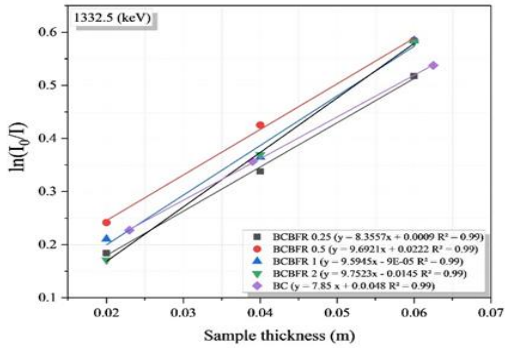

Fig. 9. The $\ln(I_0/I)$ versus sample thickness (t) at 1332.5 keV.

The data derived from Table 4 are graphed in Fig. 10 and 11. As seen in these figures, the MCNP and XCOM results are significantly similar and in a good agreement with the experimental results, based on the calculated deviations. According to the graph, the linear attenuation coefficient is increasing in higher percentages of additives. However, the trend of this increment is decreasing significantly after 0.5 percent of additives.

Moreover, the density values are illustrated in Figs. 10 and 11. Due to the higher density of basalt fiber versus bentonite (2.65 vs. 1.65 g/cm^3), it is expected that the density would increase constantly with percentages of additives; however, the density results do not follow this expectation after 0.5 percent of the additives. This could be due to a significant increase in porosity in higher additive percentages. The SEM images from the investigated mixtures illustrate in Fig. 12, prove this phenomenon.

As shown, the trend of the density values mimics the linear attenuation coefficient trend. The radiation shielding theory explains this phenomenon in which, the Compton scattering is proportional to the ratio of atomic and the mass number value of the material (Z/A), and μ~ ρZ/A (ρ is the density). The Z/A values for all the used additive materials are almost constant. As a result, it is expected that the attenuation coefficient (μ)

has a direct relation with the density of the shielding material [43].

To compare the obtained results with literatures, it can be seen that utilizing basalt fiber as an additive to bentonite increase the linear attenuation coefficient just 2 percent [23]. While, obtained results in this research indicated that adding basalt fiber and PVA resin growth the linear attenuation coefficient 14 and 24 percent in level of energy 1173 and 1332 keV, respectively.

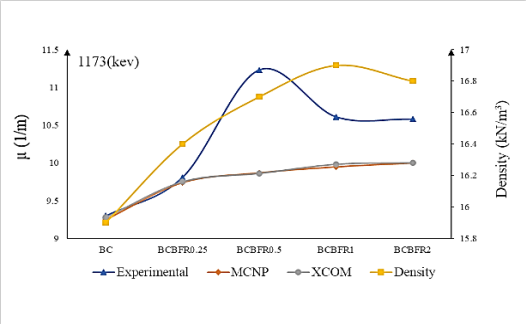

Fig. 10. The density and linear attenuation coefficient for all mixtures at 1173.2 keV.

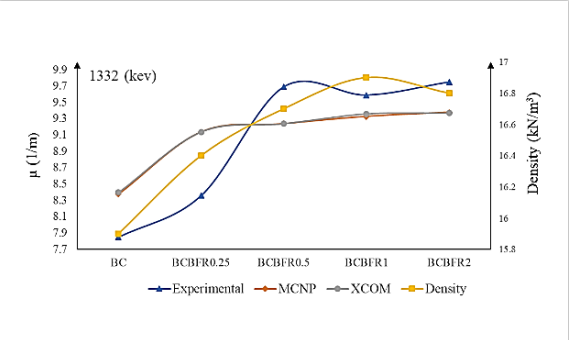

Fig. 11. The density and linear attenuation coefficient for all mixtures at 1332.5 keV.

The values of HVL and TVL are calculated according to the Eqs. (3) and (4). The results are presented in Table 5. According to the HVL and TVL values, the shielding barrier thickness significantly decreases by adding basalt fiber and PVA resin until 0.5 percent. This reduction is 20 percent in 1173.2 keV; and 23 percent in 1332.5 keV, respectively.

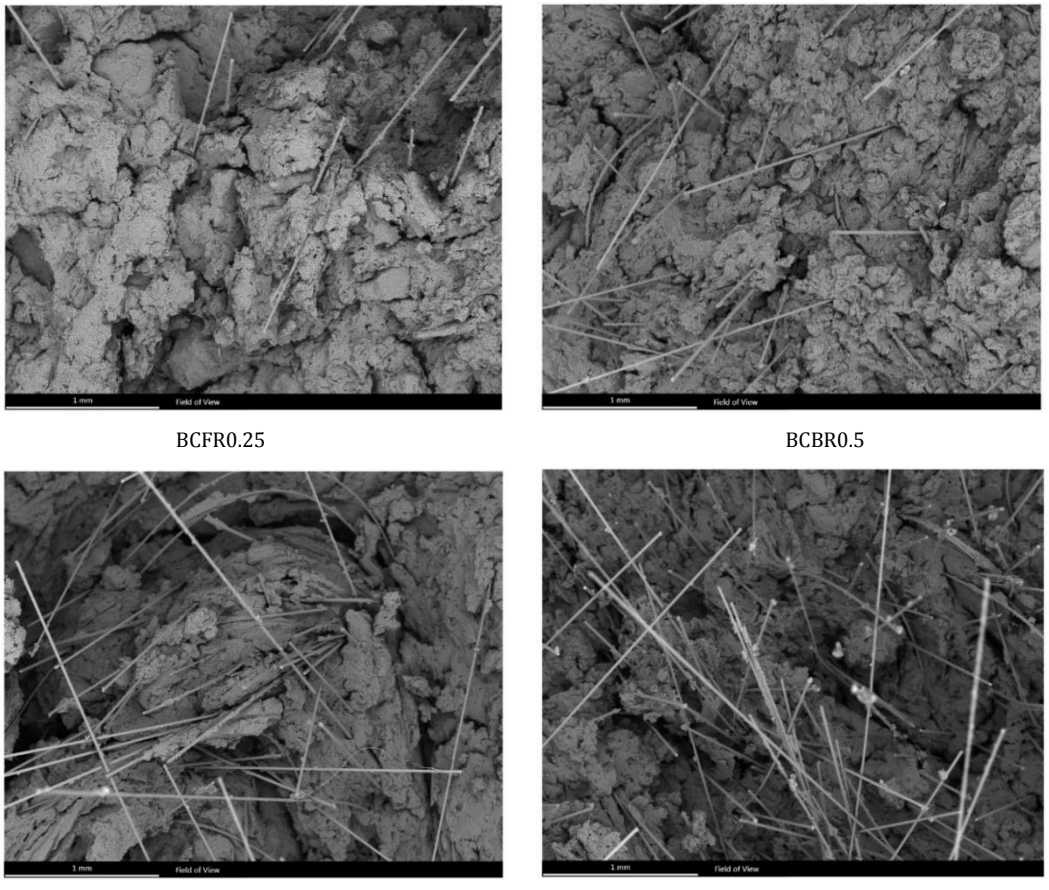

Fig. 12. SEM images of the four investigated mixtures.

Table 4. Experimental, MCNP, and XCOM results for the five samples in two studied energy levels

Sample	Energy (keV)							
	1332.5				1173.2			
	Experimental μ (1/m)	MCNP	XCOM	Deviation (%)	Experimental μ (1/m)	MCNP	XCOM	Deviation(%)
BC	7.85	8.38	8.4	6.3	9.3	9.25	9.28	0.5
BCBFR0.25	8.36	9.14	9.14	8.5	9.81	9.74	9.75	0.7
BCBFR0.5	9.69	9.24	9.24	4.9	11.23	9.87	9.86	13.8
BCBFR1	9.59	9.33	9.36	2.8	10.61	9.95	9.98	6.6
BCBFR2	9.75	9.38	9.37	3.9	10.58	10	10	5.8

Table 5. The HVL and TVL values for considered mixtures

Sample	Energy (keV)			
	1332/5		1173/2	
	HVL ($m \times 10^{-2}$)	TVL ($m \times 10^{-2}$)	HVL ($m \times 10^{-2}$)	TVL ($m \times 10^{-2}$)
BC	8/83	29/33	7/45	24/76
BCBFR0.25	8/29	27/54	7/07	23/47
BCBFR0.5	7/15	23/76	6/17	20/50
BCBFR1	7/23	24/01	6/53	21/70
BCBFR2	7/11	23/62	6/55	21/76

As noted, in addition to radiation shielding, the hydraulic and gas permeability requirements should also be satisfied for landfill cover layers. The hydraulic and gas permeability results from the tests and Eqs. 5 and 6 are plotted in Fig 13 and 14 respectively.

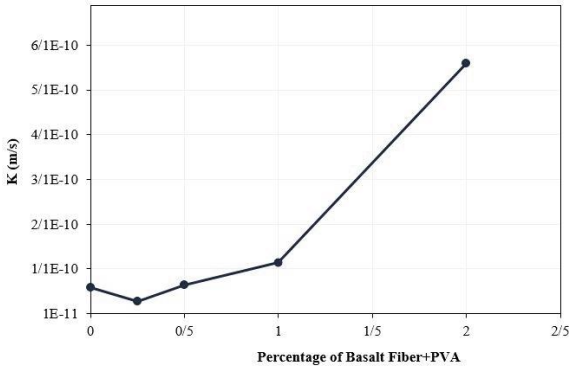

Fig. 13. Hydraulic permeability coefficient (k) for the evaluated mixture with different percentages of additives.

Fig. 13. shows a general increment in the hydraulic permeability value (k) in higher percentages of additives. This could be a result of the clay mixture inhomogeneity created by adding basalt fiber. There is a slight fluctuation for additives of less than 1 percent; however, significant growth is observed in higher values.

Fig. 14 depicts that the gas permeability decreases until 1.0 percent of additives and then drastically increases. Although in dry testing conditions, in contrast with the hydraulic permeability test, the cracks tend to extend, adding basalt fiber up to 1.0 percent would control the crack propagation, which leads to a lower gas permeability coefficient. According to the results, it seems that additives of more than 1.0 percent leads to scatter clay mixtures and cause significantly higher gas permeability. According to the United States Environmental Protection Agency (EPA) standards, the hydraulic and gas permeability of the liners should not exceed 10-9 m/sec, which are both satisfied for the recommended range of additive percentages.

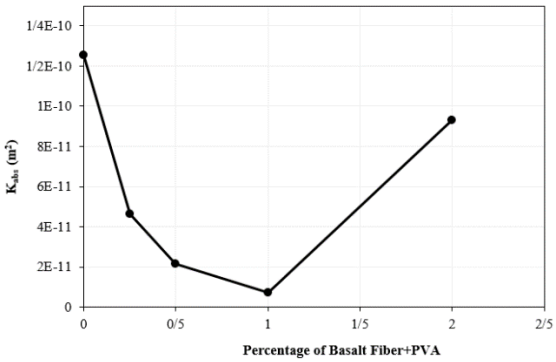

Fig. 14. Absolute gas permeability coefficient (k_{abs}) for the evaluated mixture with different percentages of additives.

5. CONCLUSION

The goal of this research was to improve the radiation shielding performance of bentonite

around low-level waste disposals by adding basalt fiber and PVA resin in four different percentages of 0.25, 0.5, 1, and 2, while the permeability is in the acceptable limit. The results show that the attenuation coefficient generally escalates up to 20% by adding 0.5 percent of basalt fiber and PVA resin, while this increment trend drops significantly in additive percentages of more than 0.5 percent. This trend mimics the density variation of the mixtures, where SEM images also prove this phenomenon by increasing the porosity of the mixtures in more than 0.5 additive percentages. Moreover, the required shielding barrier thickness, presented via HVL and TVL, is reduced by adding basalt fiber and PVA resin and stays almost constant in higher percentages. Therefore, the mixture of bentonite clay with 0.5 percent basalt fiber and PVA resin is a relatively effective low-level radiation shielding landfill cover. Moreover, by controlling the hydraulic and gas permeability of the mixtures, it could be concluded that the 0.5 to 1.0 percent of additives will keep the permeability requirement in an allowable and preferable range, according to the EPA standard ($k<10^{-9}$ m/sec).

REFERENCES

[1] Cohen, B. L. (2011). The cancer risk from low level radiation. *Radiation dose from multidetector CT.* Springer.

[2] Council, N. R. (2006). *Health risks from exposure to low levels of ionizing radiation: BEIR VII phase 2*, National Academies Press.

[3] Giusti, L. (2009). A review of waste management practices and their impact on human health. *Waste management,* 29**,** 2227-2239.

[4] Gershey, E. L., Klein, R. C., Party, E. & Wilkerson, A. 1990. Low-level radioactive waste.

[5] Francis, A. (1985). Low-level radioactive wastes in subsurface soils. *Soil reclamation processes: microbiological analyses and applications.*

[6] Holzlöhner, U., August, H. & Meggyes, T. (1997). *Advanced landfill liner systems*, Thomas Telford.

[7] Gilmore, W. R. (1977). Radioactive waste disposal: low and high level.

[8] Daniel, D. E. (1983). Shallow land burial of low-level radioactive waste. *Journal of Geotechnical Engineering,* 109**,** 40-55.

[9] Abushammala, M. F., Basri, N. E. A. & Kadhum, A. A. H. (2009). Review on landfill gas emission to the atmosphere. *European Journal of Scientific Research,* 30**,** 427-436.

[10] Tian, K., Benson, C. H. & Likos, W. J. (2016). Hydraulic conductivity of geosynthetic clay liners to low-level radioactive waste leachate. *Journal of Geotechnical and Geoenvironmental Engineering,* 142**,** 04016037.

[11] Small, J., Nykyri, M., Helin, M., Hovi, U., Sarlin, T. & Itävaara, M. (2008). Experimental and modelling investigations of the biogeochemistry of gas production from low and intermediate level radioactive waste. *Applied Geochemistry,* 23**,** 1383-1418.

[12] Alther, G. (2004). Some practical observations on the use of bentonite. *Environmental & Engineering Geoscience,* 10**,** 347-359.

[13] Kumar, S. & Yong, W.-L. (2002). Effect of bentonite on compacted clay landfill barriers. *Soil and sediment contamination,* 11**,** 71-89.

[14] Fall, M., Célestin, J. & Han, F. (2009). Suitability of bentonite-paste tailings mixtures as engineering barrier material for mine waste containment facilities. *Minerals Engineering,* 22**,** 840-848.

[15] Lee, S. & Tank, R. (1985). Role of clays in the disposal of nuclear waste: a review. *Applied clay science,* 1**,** 145-162.

[16] Sellin, P. & Leupin, O. X. (2013). The use of clay as an engineered barrier in radioactive-waste management–a review. *Clays and Clay Minerals,* 61**,** 477-498.

[17] Olukotun, S., Gbenu, S., Ibitoye, F., Oladejo, O., Shittu, H., Fasasi, M. & Balogun, F. (2018). Investigation of gamma radiation shielding capability of two clay materials. *Nuclear Engineering and Technology,* 50**,** 957-962.

[18] Singh, V. P., Badiger, N. & Kucuk, N. (2014). Gamma-ray and neutron shielding properties of some soil samples.

[19] Akbulut, S., Sehhatigdiri, A., Eroglu, H. & Çelik, S. (2015). A research on the radiation shielding effects of clay, silica fume and cement samples. *Radiation Physics and Chemistry,* 117**,** 88-92.

[20] Mann, H. S., Brar, G. S., Mann, K. S. & Mudahar, G. S. (2016). Experimental investigation of clay fly ash bricks for gamma-ray shielding. *Nuclear Engineering and Technology,* 48**,** 1230-1236.

[21] Hager, I. Z., Rammah, Y. S., Othman, H. A., Ibrahim, E. M., Hassan, S. F. & Sallam, F. H. (2019). Nano-structured natural bentonite clay coated by polyvinyl alcohol polymer for gamma rays attenuation. *Journal of Theoretical and Applied Physics,* 13**,** 141-153.

[22] Hendronursito, Y., Barus, J., Amin, M., Al Muttaqii, M., Rajagukguk, T. O., Isnugroho, K., & Birawidha, D. C. (2019). The local mineral potential from East Lampung-Indonesia: the use of basalt rock as a stone meal for cassava plant. Journal of Degraded and Mining Lands Management, 7(1), 1977.

[23] Isfahani, H. S., & Azhari, A. (2021). Investigating the effect of basalt fiber additive on the performance of clay barriers for radioactive waste disposals. Bulletin of Engineering Geology and the Environment, 80(3), 2461-2472.

[24] Dole, L. R. & Quapp, W. (2002). Radiation shielding using depleted uranium oxide in nonmetallic matrices. *ORNL/TM-2002/111, Oak Ridge National Laboratory, UT-Battelle, LLC, Oak Ridge, Tennessee (August 2002)*.

[25] Li, R., Gu, Y., Zhang, G., Yang, Z., Li, M. & Zhang, Z. (2017). Radiation shielding property of structural polymer composite: continuous basalt fiber reinforced epoxy matrix composite containing erbium oxide. *Composites Science and Technology,* 143**,** 67-74.

[26] Thyagaraj, T. & Soujanya, D. (2017). Polypropylene fiber reinforced bentonite for waste containment barriers. *Applied Clay Science,* 142**,** 153-162.

[27] Kalkan, E. (2013). Preparation of scrap tire rubber fiber–silica fume mixtures for modification of clayey soils. *Applied Clay Science,* 80**,** 117-125.

[28] Ayothiraman, R. & Singh (2017). A. Improvement of soil properties by basalt fibre reinforcement. Proc., DFI-PFSF Joint Conf. on Piled Foundations & Ground Improvement Technology for the Modern Building and Infrastructure Sector, 403-412.

[29] Moon, S., Nam, K., Kim, J. Y., Hwan, S. K. & Chung, M. (2008). Effectiveness of compacted soil liner as a gas barrier layer in the landfill final cover system. *Waste management,* 28**,** 1909-1914.

[30] Juca, J. & Maciel, F. (2006). Gas permeability of a compacted soil used in a landfill cover layer. *Unsaturated Soils..*

[31] Bergaya, F. & Lagaly, G. (2006). General introduction: clays, clay minerals, and clay science. *Developments in clay science,* 1**,** 1-18.

[32] Sim, J. & Park, C. (2005). Characteristics of basalt fiber as a strengthening material for concrete structures. *Composites Part B: Engineering,* 36**,** 504-512.

[33] Lipatov, Y. V., Gutnikov, S., Manylov, M., Zhukovskaya, E. & Lazoryak, B. (2015). High alkali-resistant basalt fiber for reinforcing concrete. *Materials & Design,* 73**,** 60-66.

[34] Li, W. & Xu, J. (2009). Mechanical properties of basalt fiber reinforced geopolymeric concrete under impact loading. *Materials Science and Engineering: A,* 505**,** 178-186.

[35] Matthys, S., Toutanji, H., Audenaert, K. & Taerwe, L. (2005). Axial load behavior of large-scale columns confined with fiber-reinforced polymer composites. *ACI Structural Journal,* 102**,** 258.

[36] Lv, Y., Wu, X., Zhu, Y., Liang, X., Cheng, Q. & Gao, M. (2018). Compression Behavior of Basalt Fiber-Reinforced Polymer Tube-Confined Coconut Fiber-Reinforced Concrete. *Advances in Materials Science and Engineering,*.

[37] Shafiq, N., Ayub, T. & Khan, S. U. (2016). Investigating the performance of PVA and basalt fibre reinforced beams subjected to flexural action. *Composite structures,* 153**,** 30-41.

[38] Kramár, S., Trcala, M., Chitbanyong, K., Král, P. & Puangsin, B. (2020). Basalt-Fiber-Reinforced Polyvinyl Acetate Resin: A Coating for Ductile Plywood Panels. *Materials,* 13**,** 49.

[39] Martin, J. E. (2006). *Physics for radiation protection: a handbook*, John Wiley & Sons.

[40] Briesmeister, J. F. (1986). MCNP: a general Monte Carlo code for neutron and photon transport. Version 3A. Revision 2. Los Alamos National Lab.

[41] Jaeger, R. (1975). Engineering Compendium on Radiation Shielding, Vol. II, Shielding Materials, S. 9.1. 12.4. Springer-Verlag, Berlin, Heidelberg, New York.

[42] Berger, M., Hubbell, J., Seltzer, S., Chang, J., Coursey, J., Sukumar, R., Zucker, D. & Olsen, K. (2016). XCOM: Photon cross sections database, 2010. *URL http://www.nist. gov/pml/data/xcom*.

[43] Krane, K. & Halliday, D. (1988). Introductory Nuclear Physics, Wi¬ ley. *New York***,** 169.